

Visualization in Bayesian workflow

Jonah Gabry

Department of Statistics and ISERP, Columbia University, New York, USA.

E-mail: jgabry@gmail.com

Daniel Simpson

Department of Statistical Sciences, University of Toronto, Canada.

Aki Vehtari

Department of Computer Science, Aalto University, Espoo, Finland.

Michael Betancourt

Department of Statistics and ISERP, Columbia University, New York, USA.

Andrew Gelman

Departments of Statistics and Political Science, Columbia University, New York, USA.

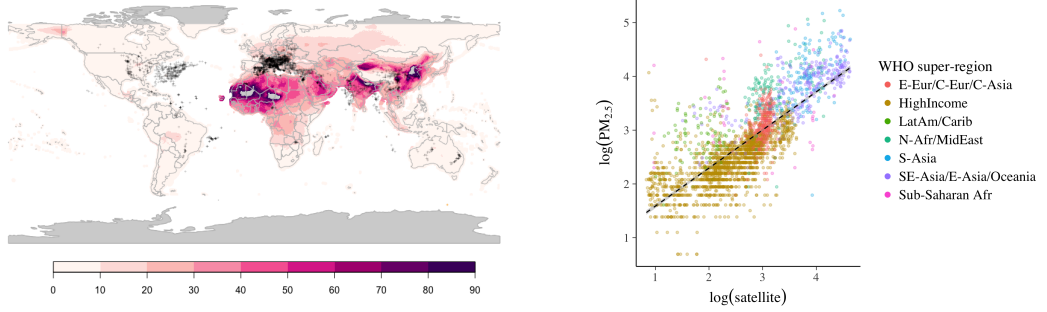
Summary. Bayesian data analysis is not only about computing a posterior distribution, and Bayesian visualization is about more than trace plots of Markov chains. Rather, practical Bayesian data analysis is an iterative process of model building, inference, model checking and evaluation, and model expansion. Visualization is not only helpful in each of these stages of the Bayesian workflow, it is indispensable for making inferences from the intricate, high-dimensional models of interest to applied researchers, and essential for understanding and diagnosing the increasingly complex algorithms required to fit such models.

1. Introduction and running example

We have found that just about every Bayesian analysis can benefit from visualizations in at least one of the following phases of the workflow: (a) Exploratory data analysis to aid in setting up an initial model; (b) Computational model checks using fake-data simulation and the prior predictive distribution; (c) Diagnosis of pathologies in Hamiltonian Monte Carlo trajectories to identify difficult geometries and motivate reparameterizations; (d) Posterior predictive checks and other juxtapositions of data and predictions under the fitted model; (e) Model comparison via tools such as cross-validation.

We consider these in the context of an applied example and discuss implementations in the `bayesplot` R package (Gabry, 2017; R Core Team, 2017), which uses `ggplot2` (Wickham, 2009) and is linked to—though not dependent on—Stan (Stan Development Team, 2017a,b), a general-purpose Hamiltonian Monte Carlo engine for Bayesian model fitting.

In order to better discuss the ways visualization can aid a statistical workflow, we consider a particular problem, the estimation of human exposure to air pollution from particulate matter measuring less than 2.5 microns in diameter ($PM_{2.5}$). Exposure to $PM_{2.5}$ is linked to a number of poor health outcomes and a recent report estimated that $PM_{2.5}$ is responsible for three million deaths worldwide each year (Shaddick et al., 2017).



(a) The satellite estimates of PM_{2.5}. The black points indicate locations of ground monitors. (b) A scatterplot of log(PM_{2.5}) vs log(satellite). The points are colored by WHO super region.

Fig. 1: *Data displays for our running example of exposure to particulate matter.*

In order to estimate the public health effect of ambient PM_{2.5}, we need a good estimate of the PM_{2.5} concentration at the same spatial resolution as our population estimates.

For our running example, we use the data from Shaddick et al. (2017) aggregated to city level to estimate ambient PM_{2.5} concentration across the world. The statistical problem is that we only have direct measurements of PM_{2.5} from ground monitors at 2980 locations, shown in Figure 1a, a sparse network with heterogeneous spatial coverage. In particular, we have especially poor coverage across Africa, central Asia, and in Russia.

In addition to the direct measure, there is a high-resolution satellite data product that converts measurements of aerosol optical depth into estimates of PM_{2.5}. The hope is that we can use the ground monitor data to calibrate the approximate satellite measurements and hence get estimates of PM_{2.5} at the required spatial resolution.

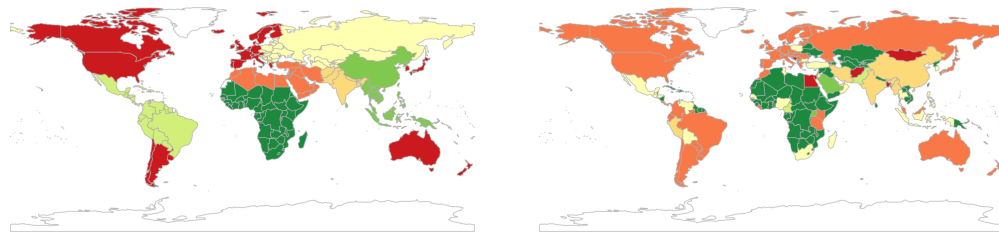
The aim of this analysis is to build a predictive model of PM_{2.5} with appropriately calibrated prediction intervals. We will not attempt a full analysis of this data, which was undertaken by Shaddick et al. (2017), but will instead focus on how visualization can be built into the statistical workflow.

2. Exploratory data analysis goes beyond just plotting the data

The most important lesson in applied statistics is to look at the data. But for complicated datasets, working out what aspects of the data to explore is more of an art than a science and it can be difficult to work out what plots will be most informative.

Plotting isn't the only way to look at the data. A more realistic workflow for building a predictive model is to use exploratory analysis to build a network of increasingly complex models (Gelman, 2004). This strategy of modeling from the ground up is particularly appropriate for modeling PM_{2.5} as we have fairly sparse data. This is a different workflow than the more “machine learning” strategy of throwing a flexible non-parametric model at the data and trying to control overfitting after the fact. Although that strategy works well in many situations, when the dataset is difficult we have found it more effective to model from the ground up.

The simplest predictive model that we can fit assumes that the satellite data product



(a) The WHO super-regions. The red region corresponds to rich countries. The remaining regions are defined based on geographic contiguity.

(b) The super-regions found by clustering. The dark green region corresponds to countries for which we have no ground monitor measurements.

Fig. 2: *World Health Organization super-regions and super-regions from clustering.*

is a good predictor of the ground monitor data after a simple linear adjustment. This was the model used by the Global Burden of Disease project prior to the 2016 update (Forouzanfar et al., 2015). Figure 1b shows a straight line that fits the data on a log-log scale reasonably well ($R^2 = 0.67$). You can also clearly see discretization artifacts at the lower values of $\text{PM}_{2.5}$.

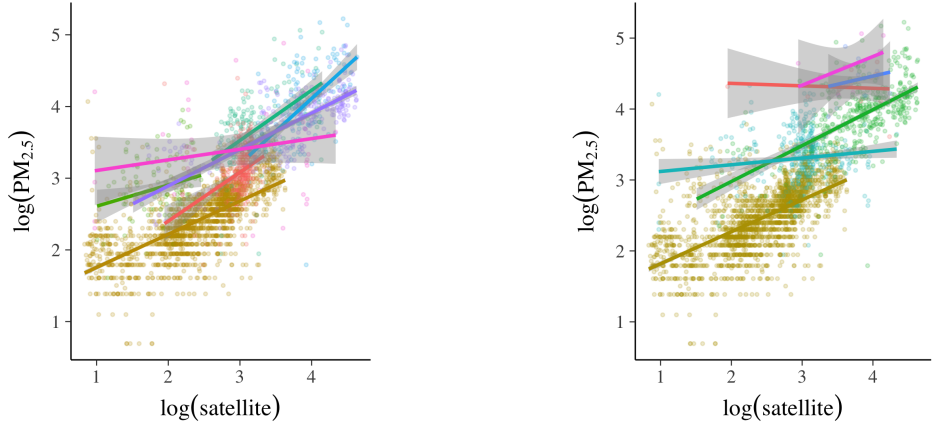
We have more information about the data than we've used. For example, we know that countries are often not exchangeable, which leads to the uncomfortable possibility that fitting only a single regression line could leave us in danger of falling prey to Simpson's paradox (that a trend can reverse when data are grouped).

We consider two possible groupings of countries. The WHO super-regions (Figure 2a) separate out rich countries and divide the remaining countries into six geographically contiguous regions. These regions have not been constructed with air pollution in mind, so we constructed a different division based on a 6-component hierarchical clustering of ground monitor measurements of $\text{PM}_{2.5}$ (Figure 2b). The seventh region constructed this way is the collection of all countries for which we do not have ground monitor data.

When the trends for each of these regions are plotted individually (Figures 3a,3b), it is clear that some ecological bias would creep into the analysis if we only used a single linear regression. We also see that some regions, particularly Sub-Saharan Africa and clusters 1 and 6, do not have enough data to comprehensively nail down the linear trend. This suggests that some borrowing of strength through a multilevel model may be appropriate.

From this preliminary data analysis, we have constructed a network of three potential models. Model 1 is a simple linear regression. Model 2 is a multilevel model where observations are stratified by WHO super-region. Model 3 is a multilevel model where observations are stratified by *clustered* super-region.

The network of models that we have grown with this exercise is smaller than it would be for a real data analysis. Shaddick et al. (2017), for example, continued this exercise to consider smaller regions and country-level variation. They also considered a spatial model for the varying coefficients. Further calibration covariates can also be included.



(a) The same as Figure 1b, but with independent linear models fitted within each WHO super-region.

(b) The same as Figure 1b, but with independent linear models fitted within each cluster region shown in Figure 2b.

Fig. 3: *Graphics in model building: here, evidence that a single linear trend is insufficient.*

3. Fake data can be almost as valuable as real data for building your model

From our exploratory data analysis, we know that a multilevel linear model where the intercept and the effect of the satellite estimates are grouped over different regions is an appropriate model for this problem. The specification of priors for multilevel models can have serious consequences for the inference (Gelman, 2006), so we need to do this carefully. In this section, we consider ways that visualization can help us set priors for these models.

Mathematically, the model will look like $y_{ij} \sim N(\beta_0 + \beta_{0j} + (\beta_1 + \beta_{1j})x_{ij}, \sigma^2)$, $\beta_{0j} \sim N(0, \tau_0^2)$, $\beta_{1j} \sim N(0, \tau_1^2)$, where y_{ij} is the logarithm of the observed PM_{2.5}, x_{ij} is the logarithm of the estimate from the satellite model, i ranges over the observations in each super-region, j ranges over the super-regions, and σ , τ_0 , τ_1 , β_0 and β_1 need prior distributions.

The key concept is that of a *generative model*, that is, the idea that when we build Bayesian models we are actually building models to generate new data. As such, our prior distributions can only be understood by considering them together with the likelihood and a prior will be good if and only if new data generated by the resulting distribution is sensible (Gelman et al., 2017). We can investigate this by plotting simulations from the full model and considering how plausible they are. We recommend generating a “flip book” of such simulations that can be used to get an idea of the variability in the data generating process.

Take, for example, some priors of the sort that are sometimes recommended as being vague: $\beta_k \sim N(0, 100)$, $\tau_k^2 \sim \text{Inv-Gamma}(1, 100)$. The data generated using these priors and shown in Figure 4a are ridiculous; note the y -axis limits and recall that the data are on the log scale. This is primarily because these priors don’t actually respect our contextual knowledge.

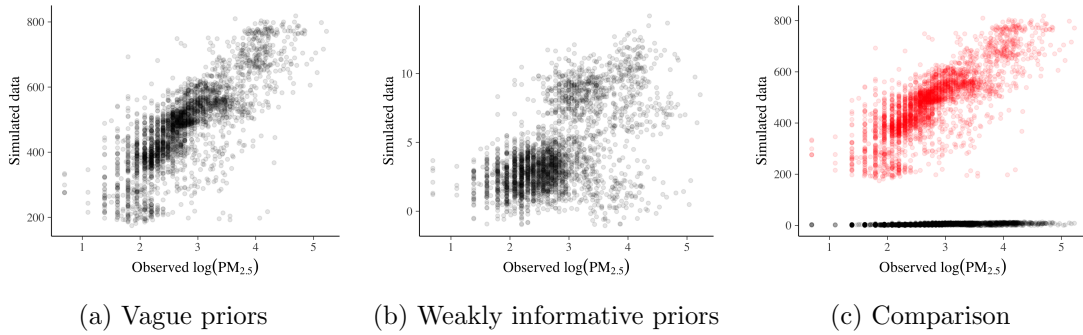


Fig. 4: (a) and (b) show realizations from the prior predictive distribution using vague priors and weakly informative priors. Simulated data are plotted on y-axis and observed data on x-axis. Panel (c) shows (a) and (b) in the same plot, with red points representing the realizations using vague priors and gray points using weakly informative priors.

We know that the satellite estimates are reasonably faithful representations of the PM_{2.5} concentration, so a more sensible set of priors would be centered around models with intercept 0 and slope 1. An example of this would be $\beta_0 \sim N(0, 1)$, $\beta_1 \sim N(1, 1)$, $\tau_k \sim N_+(0, 1)$. Data generated by this model is shown in Figure 4b. While it is clear that this realization corresponds to a quite mis-calibrated satellite model (especially when we remember that we are working on the log scale), it is quite a bit more plausible than the model with vague priors.

We argue that the tighter priors are still only *weakly* informative, in that the implied data generating process can still generate data that is much more extreme than observed data. In fact, when repeating the simulation shown in Figure 4b many times we found that the data generated using these priors can produce data points with more than $22,000 \mu\text{gm}^{-3}$, which is a stunningly high number in this context.

4. Graphical MCMC diagnostics: moving beyond trace plots

Constructing a network of models is only the first step in the Bayesian workflow. Our next job is to fit them. Once again, visualizations can be a key tool in doing this well.

Traditionally, MCMC diagnostic plots consist of trace plots and autocorrelation functions. We find these plots can be helpful to understand problems that have been caught by numerical summaries such as \bar{R} , but they are not always needed as part of workflow in the many settings where chains mix well.

For general MCMC methods it is difficult to do any better than between/within summary comparisons, following up with trace plots as needed. But if we restrict our attention to Hamiltonian Monte Carlo (HMC) and its variants, we can get much more detailed information about the performance of the Markov chain. In particular, HMC is such a well understood mathematical construct that we can construct plots that not only indicate when there is a problem, but also suggest where in the model the problem is and hence how to fix it (Betancourt, 2017).

MCMC methods that are based on local information—a broad class including Gibbs

samplers, random walk Metropolis, MALA, and HMC—work best when the posterior is, in some appropriate sense, approximately elliptical. They do not work well when the local shape of the target distribution changes rapidly throughout the parameter space. A classic example of a target distribution for which local MCMC algorithms will usually fail is Neal’s funnel distribution, where the typical set (the bulk of the target) narrows rapidly in one dimension.

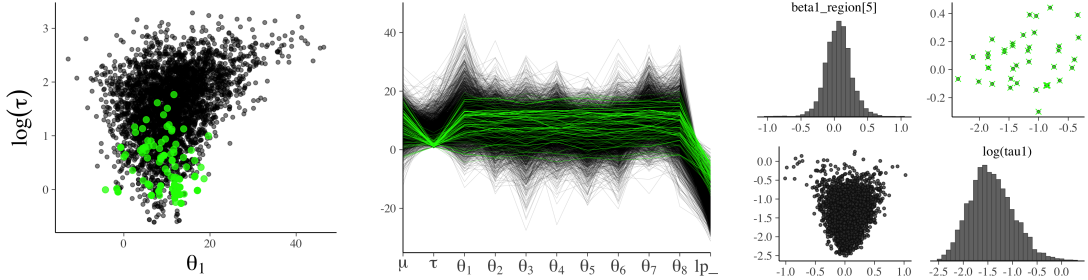
Local MCMC methods will fail to correctly resolve the funnel, and these failures typically show up as the sticking behavior discussed above, which requires long chains and careful examination of the trace plots to identify. A random-walk Metropolis Markov kernel, for example, will get stuck in the neck of the funnel, rejecting a long sequence of proposals until a rare proposal directed towards the bulk of the funnel is proposed (Betancourt and Girolami, 2015; Betancourt, 2017; Stan Development Team, 2017b).

For HMC, on the other hand, the behavior of the algorithm changes in the presence of these un-resolvable funnels. And the key to understanding why HMC is particularly sensitive for diagnosing these difficult regions is to understand how the approximate Hamiltonian dynamics work.

HMC explores the posterior through the evolution of trajectories that follow an induced Hamiltonian dynamics. In practice the numerical simulation of these Hamiltonian dynamics is achieved using a class of differential equation solvers called symplectic integrators that are specifically designed for simulating from Hamiltonian systems. They do extremely well mainly because it can be shown that while symplectic integrators do not exactly preserve the true Hamiltonian (in which case there would be no need for a Metropolis correction), they do exactly preserve a nearby Hamiltonian known as the “shadow Hamiltonian.” As long as there are no sharp changes in the geometry of the problem, the shadow Hamiltonian will be close to the true Hamiltonian (a property known as topological stability of the symplectic integrator). When, for a particular simulated trajectory, the shadow Hamiltonian moves far from the true Hamiltonian, we label the trajectory as *divergent* and label the initial point as a point of divergence.

Diagnosing divergent numerical trajectories precisely is difficult, but it is straightforward to identify these divergences heuristically by checking if the error in the Hamiltonian crosses a large threshold. Occasionally this heuristic falsely flags stable trajectories, but we can identify these false positives visually by checking if the samples generated from divergent trajectories are distributed in the same way as the non-divergent trajectories. A concentration of divergences in small neighborhoods of parameter space, however, indicates a region of high curvature in the posterior that obstructs exploration. These neighborhoods will also impede any local MCMC method, but to our knowledge only HMC has enough mathematical structure to be able to reliably diagnose these features.

There are several plots that we have found useful for diagnosing troublesome areas of the parameter space but they are more cleanly shown on a simpler multilevel model than our running example: the infamous hierarchical 8-schools problem (Rubin, 1981; Gelman et al., 2013). Figure 5a shows a scatterplot of the log standard deviation of the school-specific parameters (τ , y -axis) against the parameter representing the mean for the first school (θ_1 , x -axis). The starting points of divergent transitions, shown in green, concentrate in a particular region which is evidence of a pathology in parameter space. Figure 5b gives a different perspective on the divergences. It is a parallel coordinates



(a) Bivariate plot of the log standard deviation of the group-level coefficients (y -axis) against the mean for the first school (x -axis) in the 8-schools example. The green dots indicate starting points of divergent transitions.

(b) Parallel coordinates plot for the 8-schools example. Starting points of divergences are colored green. We can see that the divergent transitions tend to occur when τ , the standard deviation of the group-level coefficients, goes to 0.

(c) Pairs plot of the slope offset $\beta_{1,5}$ and the log of the hierarchical standard deviation τ_1 from Model 3. The divergences are isolated above the diagonal and colored green. The divergences are *not* clustered in the neck of the funnel.

Fig. 5: *Several different diagnostic plots for Hamiltonian Monte Carlo. All models were fit using the RStan interface to Stan (Stan Development Team, 2017a).*

plot including *all* parameters from the 8-schools example with divergent iterations also highlighted in green. We can see in both the bivariate plot and the parallel coordinates plot that the divergences tend to occur when the hierarchical standard deviation τ goes to 0 and the values of the θ_j 's are nearly constant.

Now that we know precisely what part of the parameter space is causing problems, we can fix it. Funnels in the parameter space can be resolved through a reparameterization that fattens out the problem area. The standard tool for fixing funnels caused by hierarchical models is moving to a non-centered parameterization, where the narrowest coordinate is made a priori independent of the other coordinates in the funnel (Betancourt and Girolami, 2015). This will typically flatten out the funnel and remove the cluster of divergences.

Turning back to our running example, Figure 5c shows a pairs plot of several parameters from our Model 3 in which the iterations ending in a divergence are plotted above the diagonal and the others below the diagonal. While the plots for the 8-schools example indicate a pathological clustering of divergences, the pairs plot for Model 3 suggests that the divergences may be false positives. Indeed, if we refit the model with a smaller step size the divergences disappear.

5. So how did we do? Posterior predictive checks are vital for model evaluation

It would be ideal to compare the model predictions to independent test data, but we can do some checking and predictive performance estimates using the data we already have. The idea behind posterior predictive checking is simple: if a model is a good fit then we should be able to use it to generate data that resemble the data we observed. This is similar in spirit to the prior checks considered in Section 3, except now we have a

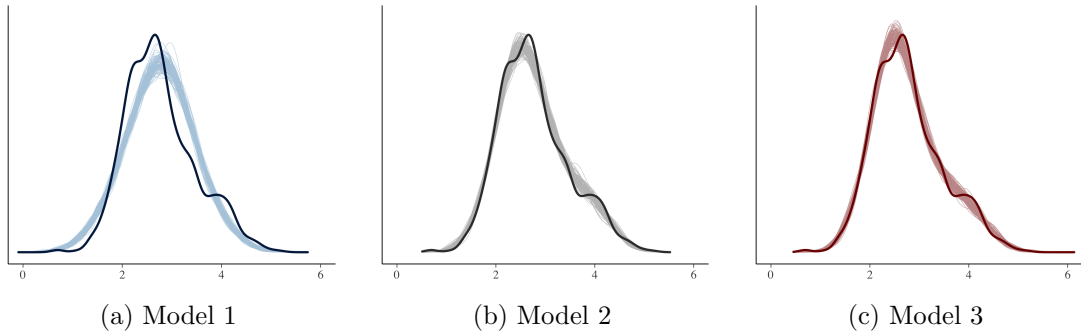


Fig. 6: *Kernel density estimate of the observed dataset y (dark curve), with density estimates for 100 simulated datasets y_{rep} drawn from the posterior predictive distribution (thin, lighter lines). These plots can be produced using `ppc_dens_overlay` in the `bayesplot` package.*

data-informed data-generating model so we can check it more stringently.

To generate the data used for posterior predictive checks (PPCs) we simulate from the posterior predictive distribution, which is the distribution of the outcome variable implied by a model after using the observed data to update our beliefs about the unknown model parameters. Posterior predictive checking is mostly qualitative, and by looking at some important features of the data and the replicated data, which were not explicitly included in the model, we may find a need to extend or modify the model.

For each of the three models, Figure 6 shows the distributions of many replicated datasets drawn from the posterior predictive distribution (thin light lines) compared to the empirical distribution of the observed outcome (thick dark line). From these plots it is evident that the multilevel models (2 and 3) are able to simulate data more similar to the observed $\log(\text{PM}_{2.5})$ values than the model without any hierarchical structure.

Posterior predictive checking makes use of the data twice, once for the fitting and once for the checking. Therefore it is a good idea to choose statistics that are orthogonal to the model parameters. If the test statistic is related to one of the model parameters, e.g., if the mean statistic is used for a Gaussian model with a location parameter, the posterior predictive checks may be less able to detect conflicts between the data and the model. Our running example uses a Gaussian model so in Figure 7 we investigate how well the posterior predictive distribution captures skewness. Model 3, which used data-adapted regions, is best at capturing the observed skewness, while Model 2 does an ok job and the linear regression (Model 1) totally fails.

We can also perform similar checks within levels of a grouping variable. For example, in Figure 8 we split both the outcome and posterior predictive distribution according to region and check the median values. The two hierarchical models give a better fit to the data at the group level, which in this case is unsurprising.

In cross-validation, double use of data is partially avoided and test statistics can be better calibrated. When performing leave-one-out (LOO) cross-validation we usually work with univariate posterior predictive distributions, and thus we can't examine properties of the joint predictive distribution. To specifically check that predictions are calibrated, the

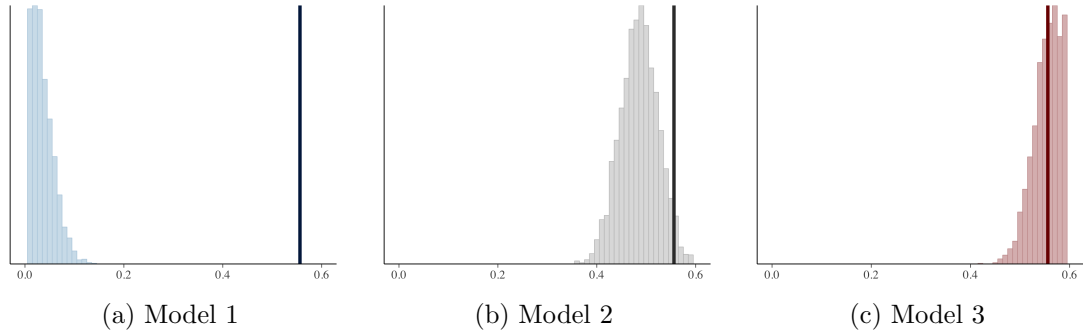


Fig. 7: *Histograms of statistics $\text{skew}(y_{\text{rep}})$ computed from 4000 draws from the posterior predictive distribution. The dark vertical line is computed from the observed data. These plots can be produced using `ppc_stat` in the `bayesplot` package.*

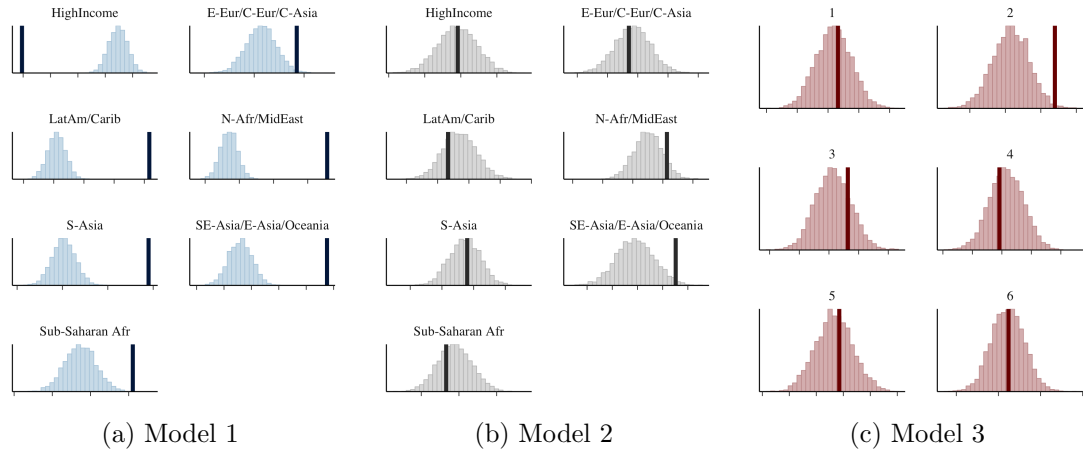


Fig. 8: *Checking posterior predictive test statistics, in this case the medians, within super-region. The vertical lines are the observed medians. These grouped plots can be made using `ppc_stat_grouped` in the `bayesplot` package.*

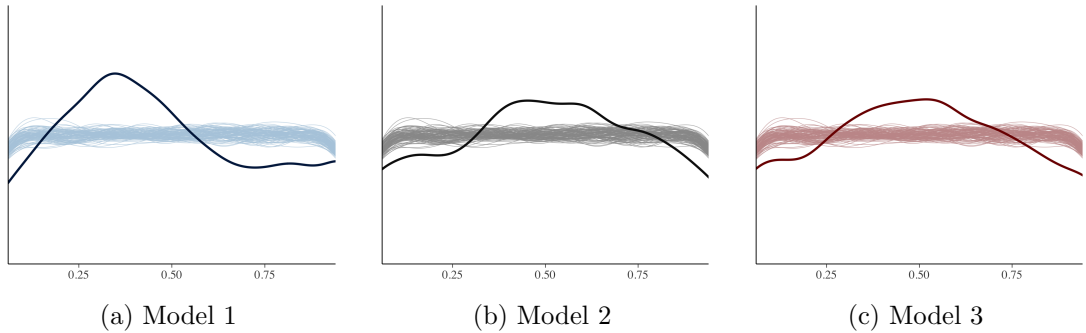


Fig. 9: *Graphical check of leave-one-out cross-validated probability integral transform (LOO-PIT). The thin lines represent simulations from the standard uniform distribution and the thick dark line in each plot is the density of the computed LOO-PITs. Similar plots can be made using `ppc_dens_overlay` and `ppc_loo_pit` in the `bayesplot` package.*

usual test is to look at the leave-one-out cross-validation predictive cumulative density function values, which are asymptotically uniform (for continuous data) if the model is calibrated (Gelfand et al., 1992; Gelman et al., 2013).

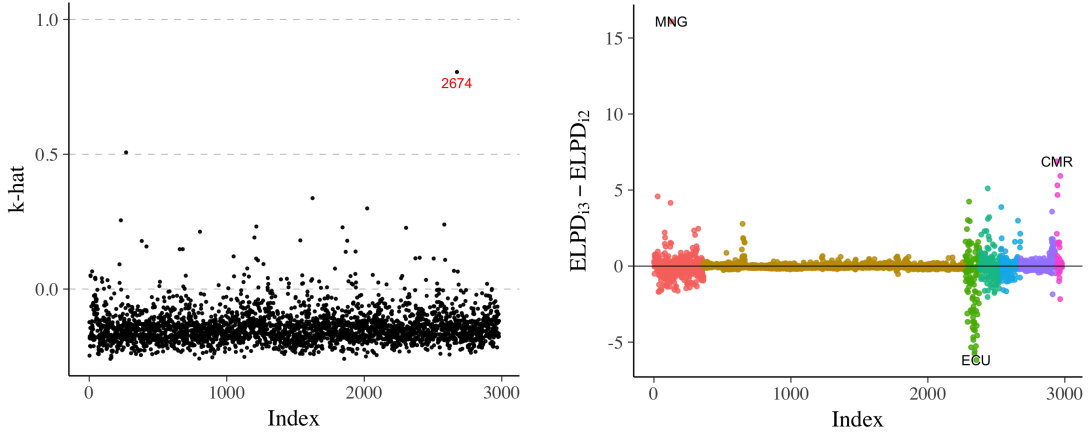
The plots shown in Figure 9 compare the density of the computed LOO-PITs (thick dark line) versus 100 simulated datasets from a standard uniform distribution (thin light lines). We can see that, although there is some clear miscalibration in all cases, the hierarchical models are an improvement over the single-level model.

The shape of the miscalibration in Figure 9 is also meaningful. The frown shapes exhibited by Models 2 and 3 indicate that the univariate predictive distributions are too broad compared to the data, which suggests that further modeling will be necessary to accurately reflect the uncertainty. One possibility would be to further sub-divide the super-regions to better capture within-region variability (Shaddick et al., 2017).

6. Pointwise plots for predictive model comparison

Cross-validation can be used to estimate the overall future predictive performance of the model, but we can also make use of the individual cross-validation marginal predictions. Gelfand et al. (1992) proposed to examine leave-one-out (LOO) log predictive density values (they called them conditional predictive ordinates) to find difficult observations to predict. Further examination of difficult to predict observations might give hints as to how to modify the model, for example, by switching from linear to nonlinear regression or switching to a more robust observation model such as Student's t instead of Gaussian or negative-binomial instead of Poisson.

In addition to looking at the individual LOO log predictive densities, it is useful to look at how influential each observation is. Some of the data points may be difficult to predict but not necessarily influential, that is, there is little difference if they are left out. One way to look at the influence is to look at the difference between log posterior predictive density and log LOO predictive density. If LOO has been computed via Pareto smoothed importance sampling (PSIS-LOO, Vehtari et al. (2016, 2017b)) as implemented in the `loo`



(a) The \hat{k} diagnostics from PSIS-LOO for Model 2. The 2674th data point is highlighted by the \hat{k} diagnostic as being influential on the posterior.

(b) The difference in pointwise ELPD values obtained from PSIS-LOO for Model 3 compared to Model 2. Positive values indicate Model 3 outperformed Model 2.

Fig. 10: Model comparisons using leave-one-out (LOO) cross validation.

package (Vehtari et al., 2017a), then we can also look at the \hat{k} diagnostic values, which are a measure of how different the posterior predictive and LOO predictive distributions are. For example, Figure 10a shows the \hat{k} diagnostics from PSIS-LOO for our Model 2. The 2674th data point is highlighted by the \hat{k} diagnostic as being influential on the posterior. If we examine the data we find that this point is the only observation from Mongolia and corresponds to a measurement $(x, y) = (\log(\text{satellite}), \log(\text{PM}_{2.5})) = (1.95, 4.32)$, which would look like an outlier if highlighted in the scatterplot in Figure 1b. By contrast, under Model 3 the \hat{k} value for the Mongolian observation is significantly lower ($\hat{k} \approx 0.5$) indicating that that point is better resolved in Model 3.

It is common to find in cross-validation that a left-out observation that is difficult to predict with one model is difficult to predict with another model. The more similar the compared models are, the more similar the predictions are, which makes it useful to look at pairwise differences in predictive accuracy for each observation. Figure 10b shows the difference between the expected log predictive densities (ELPD) for the individual data points estimated using PSIS-LOO. Model 3 appears to be slightly better than Model 2, especially for difficult observations like Mongolia.

7. Discussion

Visualization is probably the most important tool in an applied statistician's toolbox and is an important complement to quantitative statistical procedures. In this paper, we've demonstrated that it can be used as part of a strategy to compare models, to identify ways in which a model fails to fit, to check how well our computational methods have resolved the model, to understand the model well enough to be able to set priors, and to actually build the model.

The last of these tasks is a little bit controversial as we are using the data to model the data. A serious concern in this case is that the resulting models will generalize poorly to new datasets. In the visual workflow we've outlined in this paper we have done this in two places. In Section 3 we proposed prior predictive checks with the recommendation that the data generating mechanism should be broader than the distribution of the observed data in line with the principle of weakly informative priors. In Section 5 we recommended undertaking careful calibration checks as well as checks based on summary statistics.

There are other criticisms to using the observed data to build a model. A lot of the taboo around using the data twice comes from ideas around hypothesis testing and unbiased estimation, which we think have severe problems beyond anything that we are proposing (Gelman and Loken, 2014). Hence, we are of the opinion that the danger of overfitting the data described in the previous is much more concerning.

Regardless of concerns we have about using the data twice, the workflow that we have described in this paper (perhaps without the stringent prior and posterior predictive checks) is common in applied statistics. As academic statisticians, we have a duty to understand the consequences of this workflow and offer concrete suggestions to robustify practice. We firmly believe that theoretical statistics should be the theory of applied statistics, otherwise it's just the tail trying to wag the dog.

Acknowledgements

The authors thank Gavin Shaddick and Matthew Thomas for their help with the PM_{2.5} example, Ari Hartikainen for suggesting the parallel coordinates plot, and the Sloan Foundation, Columbia University, U.S. National Science Foundation, Institute for Education Sciences, and Office of Naval Research for financial support.

References

Betancourt, M. (2017). A conceptual introduction to Hamiltonian Monte Carlo. arXiv preprint arxiv:1701.02434.

Betancourt, M. and M. Girolami (2015). Hamiltonian Monte Carlo for hierarchical models. In S. K. Upadhyay, U. Singh, D. K. Dey, and A. Loganathan (Eds.), *Current Trends in Bayesian Methodology with Applications*, pp. 79–101. Chapman & Hall. arXiv:1312.0906.

Forouzanfar, M. H., L. Alexander, H. R. Anderson, V. F. Bachman, S. Biryukov, M. Brauer, R. Burnett, D. Casey, M. M. Coates, A. Cohen, et al. (2015). Global, regional, and national comparative risk assessment of 79 behavioural, environmental and occupational, and metabolic risks or clusters of risks in 188 countries, 1990–2013: a systematic analysis for the Global Burden of Disease Study 2013. *The Lancet* 386(10010), 2287–2323.

Gabry, J. (2017). *bayesplot*: Plotting for Bayesian models. R package version 1.3.0, <http://mc-stan.org/bayesplot>.

Gelfand, A. E., D. K. Dey, and H. Chang (1992). Model determination using predictive distributions with implementation via sampling-based methods (with discussion). In J. M. Bernardo, J. O. Berger, A. P. Dawid, and A. F. M. Smith (Eds.), *Bayesian Statistics 4*, pp. 147–167. Oxford University Press.

Gelman, A. (2004). Exploratory data analysis for complex models. *Journal of Computational and Graphical Statistics* 13(4), 755–779.

Gelman, A. (2006). Prior distributions for variance parameters in hierarchical models (comment on article by Browne and Draper). *Bayesian analysis* 1(3), 515–534.

Gelman, A., J. B. Carlin, H. S. Stern, D. B. Dunson, A. Vehtari, and D. B. Rubin (2013). *Bayesian Data Analysis* (Third ed.). Chapman & Hall/CRC. Chapter 6, Section “Marginal predictive checks”.

Gelman, A. and E. Loken (2014). The statistical crisis in science: Data-dependent analysis-a “garden of forking paths”-explains why many statistically significant comparisons don’t hold up. *American Scientist* 102(6), 460.

Gelman, A., D. Simpson, and M. Betancourt (2017). The prior can generally only be understood in the context of the likelihood. *arXiv preprint arXiv:1708.07487*.

R Core Team (2017). *R: A Language and Environment for Statistical Computing*. Vienna, Austria: R Foundation for Statistical Computing.

Rubin, D. B. (1981). Estimation in parallel randomized experiments. *Journal of Educational Statistics* 6, 377–401.

Shaddick, G., M. L. Thomas, A. Green, M. Brauer, A. Donkelaar, R. Burnett, H. H. Chang, A. Cohen, R. V. Dingenen, C. Dora, et al. (2017). Data integration model for air quality: a hierarchical approach to the global estimation of exposures to ambient air pollution. *Journal of the Royal Statistical Society: Series C (Applied Statistics)* Available online 13 June 2017. arXiv:1609.00141.

Stan Development Team (2017a). RStan: the R interface to Stan, version 2.16.1. <http://mc-stan.org>.

Stan Development Team (2017b). *Stan Modeling Language User’s Guide and Reference Manual, Version 2.16.0*. <http://mc-stan.org>.

Vehtari, A., A. Gelman, and J. Gabry (2016). Pareto smoothed importance sampling. *arXiv preprint arXiv:1507.02646*.

Vehtari, A., A. Gelman, and J. Gabry (2017a). loo: Efficient leave-one-out cross-validation and WAIC for Bayesian models. R package version 1.0.0, <http://mc-stan.org/loo>.

Vehtari, A., A. Gelman, and J. Gabry (2017b). Practical Bayesian model evaluation using leave-one-out cross-validation and WAIC. *Statistics and Computing* 27(5), 1413–1432. arXiv:1507.04544.

Wickham, H. (2009). *ggplot2: Elegant Graphics for Data Analysis*. Springer-Verlag New York.